Inorganic Chemistry

ARTICLE

pubs.acs.org/IC

Coordination Polymers of Hexacyanotrimethylenecyclopropanediide and Its Monoanionic Radical: Synthesis, Structure, and Magnetic Properties

Anna M. Kutasi, David R. Turner, Paul Jensen, Boujemaa Moubaraki, Stuart R. Batten,* and Keith S. Murray*

School of Chemistry, Monash University, Clayton, Victoria 3800, Australia

Supporting Information

ABSTRACT: The first examples of polymeric complexes that contain the polynitrile dianion hexacyanotrimethylenecyclopropanediide ($HCTMCP^{2-}$) were isolated and their magnetic properties have been explored. Complexes of the form $(n\text{-TBA})_2[M(HCTMCP)_2(H_2O)_2]$ (**1**) (M = Mn^{II}, Fe^{II}, Co^{II}, Cd^{II}) possess (4,4) sheet structures with large cavities that contain the tetra-*n*-butylammonium (*n*-TBA) countercations. Synthesis using sodium as the countercation yields a family of products with the general form $[M(S)_4M(S)_2(HCTMCP)_2]$ (S = EtOH, M = Fe^{II} (**2**); S = MeOH, M = Co^{II} or Zn^{II} (**3**)). These complexes adopt a variety of two-dimensional (2D) structures. The complex $[Mn_3(HCTMCP)_2(H_2O)_{12}](HCTMCP)\cdot 6(H_2O)$ (**4**) contains cationic (6,3) sheets with the counteranion and solvent molecules encapsulated within the hexagonal windows. Complexes **1**−**4** display weak antiferromagnetic coupling in all cases. The first example of a complex that contains the CN-coordinated monoanionic radical $HCTMCP^{\bullet-}$, $[Cu(HCTMCP)(MeCN)_2]$ (**5**) is described. This one-dimensional (1D) coordination polymer, containing tetrahedral Cu^{I} centers, displays medium strength antiferromagnetic coupling that is mediated through π-interactions between the radical anions on adjacent chains.

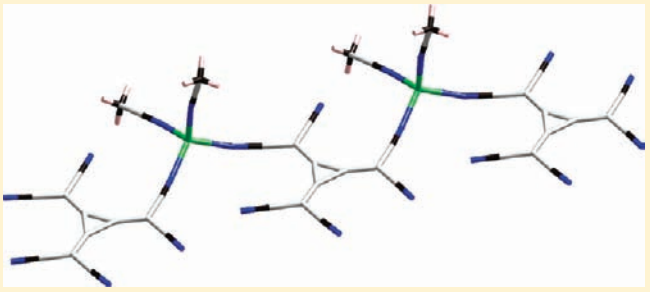

INTRODUCTION

Coordination polymers that contain nitrile-donor ligands have been an active area of research interest for many years.[1] The first known example of a CN-containing coordination polymer was Prussian blue, discovered accidently in the early 18th century but not characterized for a further 200 years, with structural characterization occurring later still.[1b,c] Since the first low-temperature magnetic studies of Prussian blue analogues[1d,e] there have been many more reported examples of such materials showing either ferri- or ferromagnetic behavior with high ordering temperatures.[1f−i] The chemistry of cyano bridges has been further expanded by the use of hexacyanometallates in combination with coordinatively unsaturated transition metal chelate complexes to generate bimetallic compounds with reduced symmetry compared to the cubic Prussian blue networks.[2]

The nonlinear bridging ligands dicyanamide, dca $[N(CN)_2]^-$, and tricyanomethanide, tcm $[C(CN)_3]^-$, were first used in the 1960s[3] with the first reports of long-range magnetic ordering in such systems occurring 30 years later.[4] For example, dca complexes have been shown to display ferromagnetic ordering (Co^{II}, Ni^{II}, and Cu^{II})[4c,d,g] and spin-canted antiferromagnetic behavior (Cr^{II}, Mn^{II}, and Fe^{II}).[4e,h] In binary dca systems such as $[M(dca)_2]$, the dicyanamide ligand coordinates in a $\mu_{1,3,5}$ manner in which all of the nitrogen atoms are coordinated to a metal, allowing access to M-NCN-M magnetic exchange pathways. Other examples containing this ligand binding mode in complexes that contain neutral coligands also display long-range ordering, for example, $\{[M(dca)_2(H_2O)]\cdot phz\}$ (phz = phenazine; M = Co, Ni).[4f] The use of larger polycyano species such as 2-dicyanomethylene-1,1,3,3-tetracyanopropanediide (tcpd), 1,1,2,4,5,5-hexacyano-3-aza-penta-1,4-dienide (hcazpd), 2,2-dicyano-1-ethoxyethenolate (dcne), dicyanonitrosomethanide (dcnm), and *N*,7,7-tricyanoquinomethanimine (TCQMI) has also been reported.[5] For example, polymeric complexes of the form $[M(dcne)_2(H_2O)_2]$ (M = Mn^{II}, Fe^{II}) display weak antiferromagnetic coupling between metal centers.

Organic, polycyano radical anions have also been used to great effect in the construction of coordination polymers with magnetically coupled pathways. The radical anions that have attracted most interest, and are of particular relevance to the present study, are tetracyanoethylene ($tcne^{\bullet-}$) and 7,7,8,8-tetracyano-*p*-quinodimethane ($tcnq^{\bullet-}$).[6] Recent d- and f-block work on these radical ligands, and on ring-substituted $(tcnqR_2)^{\bullet-}$ analogues, has yielded valuable information on magnetic ordering and structural details, such as M-NC bonding/bridging modes and crystal packing arrangements, the latter including one-dimensional (1D) chains, two-dimensional (2D) layer motifs, or three-dimensional (3D) networks. Some highlights, that are by no means exhaustive, include (i) a review of the latest findings on the high-T_C

Received: March 23, 2011
Published: June 15, 2011

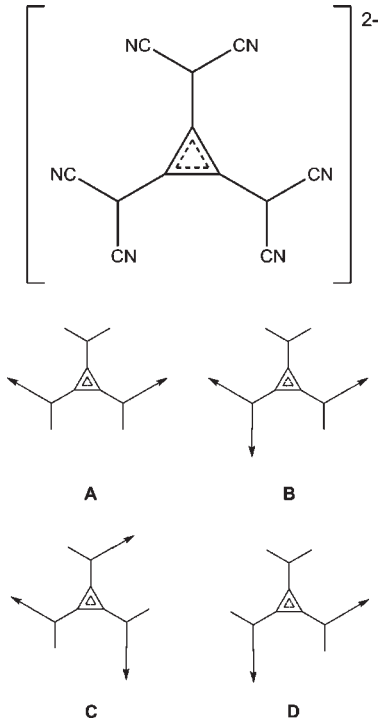

Figure 1. Dianion hexacyanotrimethylenecyclopropanediide ($HCTMCP^{2-}$) shown in a delocalized form. The species also exists as a monoanionic radical, $HCTMCP^{\bullet-}$. The binding modes of the ligands are shown schematically as observed in complexes **1** (A), **2** and **3** (B), **4** (C), and **5** (D).

magnet, $[V^{II}(tcne^{\bullet-})_x(tcne^{2-})_{1-x/2}]$,[7] involving μ_4-tcne bridging (ii) structure and magnetic ordering of the 3D materials $[Mn^{II}(tcne^{\bullet-})_{3/2}](I_3)_{1/2}$, prepared from $Mn^{II}I_2(thf)_3$ plus tcne, comparisons being made to the related compound $[Mn(tcne^{\bullet-})(C_4(CN)_8^{2-})_{1/2}].0.74CH_2Cl_2$,[8] (iii) covalently bridged 2D networks in $[Ru^{II}_2(O_2CCF_3)_4(tcnqR_2^{\bullet-})]$[9] and stepwise, neutral-ionic phase transitions in a donor−acceptor chain compound $[Ru_2(2,3,5,6\text{-}F_4\text{-}PhCO_2)_4(dmdcnqi^{\bullet-})]$, where 2,3,5,6-$F_4$-$PhCO_2$ is 2,3,5,6-tetrafluorobenzoate and $dmdcnqi^{\bullet-}$ = 2,5-dimethyl-N,N′-dicyanoquinonediimine radical anion,[10] and (iv) monomeric, mixed-spin species $[Ln(tcnqF_4^{\bullet-})_2(H_2O)_x].(tcnqF_4^{\bullet-})(3H_2O)$, where x = 6 or 7 and the Sm, Gd, and Dy members show low temperature magnetic ordering.[11]

Our interest has recently turned to the organo-polycyano species hexacyanotrimethylenecyclopropanediide ($HCTMCP^{2-}$), which is also known in its monoanionic radical form ($HCTMCP^{\bullet-}$).[12] The anion is planar with six nitrile groups projecting from the radialene-type core (Figure 1). The $HCTMCP^{2-}$ dianion has been used primarily in the preparation of novel donor−acceptor salts. The first such compounds were of the form $[(\eta^6\text{-}C_6Me_3H_3)_2M][HCTMCP]$ or $[(\eta^6\text{-}C_6Me_6)_2M][HCTMCP]$ (M = Fe, Ru) in which stacks of alternating cations and anions display donor−acceptor charge transfer (CT) behavior.[12a] CT salts have also been reported that contain the $HCTMCP^{\bullet-}$ radical anion with the structure containing segregated, infinite stacks of both the cations and the anions.[12b] Stacks of the radical anion have also been reported in electron transfer salts of $[Fe(C_5Me_5)_2]^+(HCTMCP)^{\bullet-}$ with antiferromagnetic coupling occurring along both the cationic and anion chains.[12c]

Our aims in this current work were to incorporate the $HCTMCP^{2-}$ dianion and the $HCTMCP^{\bullet-}$ radical into coordination polymers with first-row transition metals, whereby the polycyano species is σ-bonded to the metal ions through the nitrile arms. A key aim was to see if long-range magnetically ordered materials could be obtained. The divergent nature of the potentially coordinating nitrile groups, that are unable to chelate, lends itself well to the formation of polymeric complexes in combination with "naked" metal ions. The symmetry and directions of the CN arms in HCMTCP are different to those observed, to date, in tcne, tcnq, and dmdcnqi coordination polymers, summarized above. The bridging mode **D** in Figure 1 is rather similar to that of the noncyclic polycyano ligand, $C_3(CN)_5^-$, observed in the 1D tetraphenylporphyrin complex $[Mn^{III}TPP(\mu_2\text{-}C_3(CN)_5)]$.[13] Herein we report the synthesis of eight novel, 2D coordination polymers containing the $HCTMCP^{2-}$ dianion which display weak antiferromagnetic communication between the metal centers. A 1D Cu^I complex containing the μ_2-$HCTMCP^{\bullet-}$ monoanionic bridging unit is also described. These are the first reported examples of the HCTMCP species being incorporated into coordination frameworks. Attempts to make other M−HCTMCP$^{\bullet-}$ compounds with M^{II} having intrinsic spin, such as Mn, Fe, and Co, were unsuccessful.

EXPERIMENTAL SECTION

General Procedures. All reagents were purchased from standard commercial sources and were used as received. Solvents were either of reagent grade or analytical grade (for spectroscopic measurements) and were used without further purification. All reactions were performed in a standard aerobic atmosphere. $(n\text{-TBA})_2(HCTMCP)$, $Na_2(HCTMCP)$, and $K^+(HCTMCP^{\bullet-})$ were synthesized according to literature procedures.[14] IR spectra were collected as KBr discs using a Perkin-Elmer 1600 series FTIR spectrometer. Microanalyses were conducted at the Campbell Analytical Laboratory, University of Otago, New Zealand.

Syntheses. *$(n\text{-TBA})_2[Mn(HCTMCP)_2(H_2O)_2]$ (**1Mn**).* A methanolic solution (5 mL) of $Mn(NO_3)_2\cdot 6H_2O$ (30 mg, 0.12 mmol) was mixed with an acetonitrile solution (5 mL) of $[(n\text{-TBA})_2(HCTMCP)]$ (73 mg, 0.10 mmol). The clear solution was left to stand. After standing for 24 h, well-formed pale yellow irregular cubic crystals appeared. These were filtered and washed several times with small amounts of methanol and dried in air (Yield 50 mg, 49%). IR (ν/cm^{-1}): 3376mbr, 2966 m, 2201s, 2177s, 1657w, 1408s, 1134w, 1028w, 882w, 700w, 562 m. Anal. Calcd. (found) for $C_{56}H_{76}CoN_{14}O_2$: C, 65.10 (66.45); H, 7.36 (8.06); N, 18.98 (18.73).

*$(n\text{-TBA})_2[Fe(HCTMCP)_2(H_2O)_2]$ (**1Fe**).* A methanolic solution (5 mL) of $Fe(BF_4)_2\cdot 6H_2O$ (39 mg, 0.12 mmol) was mixed with an acetonitrile solution (5 mL) of $[(n\text{-TBA})_2(HCTMCP)]$ (81 mg, 0.11 mmol). A pale blue solution formed. This was filtered and left to stand. After standing at room temperature for one day colorless crystals appeared. These were filtered and washed several times with small amounts of methanol and dried in air (Yield 67 mg, 59%). IR (ν/cm^{-1}): 3361sbr, 2967 m, 2876w, 2200s, 2178s, 1408s, 1134w, 1009w, 883w, 741vw, 561 m. Anal. Calcd. (found) for $C_{56}H_{76}FeN_{14}O_2$: C, 65.04 (65.36); H, 7.36 (7.13); N, 18.97 (18.99).

*$(n\text{-TBA})_2[Co(HCTMCP)_2(H_2O)_2]$ (**1Co**).* A methanolic solution (5 mL) of $Co(NO_3)_2\cdot 6H_2O$ (32 mg, 0.11 mmol) was mixed with an acetonitrile solution (5 mL) of $[(n\text{-TBA})_2(HCTMCP)]$ (85 mg, 0.12 mmol). A yellow precipitate formed immediately. This was filtered, and the remaining pink solution was left to stand. After a few hours the pink solution changed to a pale blue solution. After standing at room temperature for 4 days, well-formed cubic yellow crystals appeared. These were filtered and washed several times with small amounts of methanol and dried in air (Yield 35 mg, 31%). IR (ν/cm^{-1}): 3386mbr, 3304mbr, 2968 m, 2877w, 2202s, 2179s, 1674w, 1487 msh, 1409s, 1256w, 1135w, 1110w, 1030w,

dx.doi.org/10.1021/ic200591u |*Inorg. Chem.* 2011, 50, 6673–6684

884w, 803w, 744w, 562 m. Anal. Calcd. (found) for $C_{56}H_{76}CoN_{14}O_2$: C, 64.85 (65.85); H, 7.33 (7.37); N, 18.91 (19.14).

(n-TBA)$_2$[Cd(HCTMCP)$_2$(H$_2$O)$_2$] (**1Cd**). A methanolic solution (5 mL) of $Cd(NO_3)_2 \cdot 6H_2O$ (36 mg, 0.12 mmol) was mixed with an acetonitrile solution (5 mL) of [(n-TBA)$_2$(HCTMCP)] (78 mg, 0.12 mmol). The colorless solution was left to stand. After standing at room temperature for several days, well-formed colorless irregular blocks appeared. These were filtered and washed several times with small amounts of methanol and dried in air (Yield 47 mg, 36%). IR (ν/cm^{-1}): 3374mbr, 2966 m, 2876w, 2202s, 2179s, 1663w, 1487 msh, 1410s, 1254w, 1134w, 1110w, 1028w, 882w, 801w, 740w, 562 m. Anal. Calcd. (found) for $C_{56}H_{76}CdN_{14}O_2$: C, 61.67 (61.74); H, 6.97 (6.91); N, 17.99 (18.02).

[Fe(EtOH)$_4$Fe(EtOH)$_2$(HCTMCP)$_2$] (**2**). A solution of $Fe(ClO_4)_2 \cdot 6H_2O$ (188 mg, 0.74 mmol) and a pinch of ascorbic acid in 5 mL of ethanol were added to an aqueous solution (5 mL) of Na_2(HCTMCP) (149 g, 0.54 mmol). The resulting colorless solution was filtered and left to stand. After several days, colorless needles formed. The mother liquor was decanted, and the crystals were washed with ethanol, and then collected by filtration (Yield 80 mg, 18%). IR (ν/cm^{-1}): 3422sbr, 2215s, 2187s, 1628 m, 1443s, 1141w, 1042vw, 877vw, 707vw, 562 m. Anal. Calcd. (found) for $C_{36}H_{36}FeN_{12}O_6$: C, 51.16 (51.62); H, 4.26 (3.96); N, 19.89 (20.09).

[Co(MeOH)$_4$Co(MeOH)$_2$(HCTMCP)$_2$] (**3Co**). A solution of $Co(NO_3)_2 \cdot 6H_2O$ (191 mg, 0.66 mmol) in 5 mL of methanol was added to an aqueous solution (5 mL) of Na_2(HCTMCP) (145 mg, 0.53 mmol). The resulting bright orange solution was filtered and left to stand. After several days, orange rods formed. The mother liquor was decanted, and the crystals were washed with methanol, and then collected by filtration (Yield 87 mg, 22%). IR (ν/cm^{-1}): 3423sbr, 2213s, 2180s, 1720vw, 170vw, 1644 m, 1638vw, 1425s, 1137w, 1017vw, 709vw, 562 m. Anal. Calcd. (found) for $C_{30}H_{24}Co_2N_{12}O_6$: C, 46.97 (46.98); H, 3.13 (3.25); N, 21.92 (22.09).

[Zn(MeOH)$_4$Zn(MeOH)$_2$(HCTMCP)$_2$] (**3Zn**). A solution of $Zn(ClO_4)_2 \cdot 6H_2O$ (186 mg, 0.5 mmol) in 5 mL of methanol was added to an aqueous solution (5 mL) of Na_2(HCTMCP) (137 mg, 0.5 mmol). The resulting colorless solution was filtered and left to stand. After several days, colorless rods formed. The mother liquor was decanted, and the crystals were washed with methanol, and then collected by filtration (Yield 92 mg, 24%). IR (ν/cm^{-1}): 3437 m, 2229s, 2206s, 2171ssh, 1638 m, 1429s, 1141 m, 1008vw, 710vw, 563 m. Anal. Calcd. (found) for $C_{30}H_{24}Zn_2N_{12}O_6$: C, 46.55 (46.69); H, 3.08 (3.37); N, 21.56 (21.87).

[Mn$_3$(HCTMCP)$_2$(H$_2$O)$_{12}$]HCTMCP·6H$_2$O (**4**). A solution of $Mn(NO_3)_2 \cdot 4H_2O$ (135 mg, 0.54 mmol) in 5 mL of methanol was added to an aqueous solution (5 mL) of Na_2(HCTMCP) (152 mg, 0.55 mmol). The resulting colorless solution was filtered and left to stand. After several days, colorless irregular blocks formed. The mother liquor was decanted, and the crystals were washed with methanol, and then collected by filtration (Yield 102 mg, 16%). IR (ν/cm^{-1}): 3474 m, 2214s, 2183s, 1638w, 1427s, 1137 m, 1011vw, 708vw, 563 m. Anal. Calcd. (found) for $Mn_3C_{36}H_{36}N_{18}O_{18}$: C, 36.82 (36.54); H, 3.07 (2.98); N, 21.48 (21.54).

[Cu^I(HCTMCP)(MeCN)$_2$] (**5**). A 5 mL methanol solution containing $Cu(ClO_4)_2 \cdot 6H_2O$ (46 mg, 0.126 mmol) was allowed to diffuse slowly into an MeCN/MeOH (2:1) solution containing K^+(HCTMCP$^{\bullet-}$) (67 mg, 0.25 mmol). After standing at room temperature for several days dark blue, irregular blocks appeared. These were recovered by filtration, washed several times with small amounts of methanol, and dried in air (Yield 26 mg, 56%). IR (KBr disk, ν/cm^{-1}): 2218s, 2190 msh, 1422 m, 1250w, 1139, 1091vw, 624, 560 m. Anal. Calc. (found) for $C_{16}H_6CuN_8$: C, 51.36 (51.48); H, 1.61 (1.68); N, 29.96 (30.04).

X-ray Crystallography. Data were collected using a Nonius KappaCCD diffractometer equipped with graphite monochromated Mo−Kα radiation (λ = 0.71073 Å). Data collection temperatures were maintained at 123 K using an open-flow N_2 cryostream. Integration was carried out using the program DENZO-SMN and data were corrected for Lorentz polarization effects and for absorption using the program SCALEPACK.[15] Solutions were obtained by direct methods (SHELXS 97).[16] Refinement against F^2 was carried out using full matrix least-squares (SHELXL 97)[16] with the aid of the graphical interface program X-Seed.[17] All hydrogen atoms attached to carbon were included in the model at idealized positions and refined using a riding model. Where possible hydrogen atoms attached to oxygen were located from the Fourier difference map and allowed to refine freely (exceptions to this are detailed in Table 1). Crystallographic data for complexes **1**−**5** are listed in Table 1. Full crystallographic data for **1**−**5** are available on request from the Cambridge Crystallographic Data Centre, 12 Union Road, Cambridge, CB2 1EZ, U.K. (http://www.ccdc.cam.ac.uk/). CCDC deposition numbers 818313−818321.

Magnetic Susceptibility Measurements. Direct current (DC) susceptibilities were measured using a Quantum Design MPMS 5 SQUID magnetometer calibrated by the use of a standard palladium sample (Quantum Design) of an accurately known magnetization or by use of magnetochemical calibrants such as $CuSO_4 \cdot 5H_2O$ and $[Ni(en)_3]S_2O_3$. Samples were contained in gelatin capsules held at the end of a drinking straw which was fixed to the end of the sample rod. For alternating current (AC) measurements a field of 3.5 Oe was used oscillating at 20 Hz. Compounds containing anisotropic Co^{II} or Fe^{II} ions, formally with T ground states, were dispersed in Vaseline to eliminate temperature dependent crystallite orientation effects. Magnetization measurements, in field-cooled (FCM); (5 Oe) and zero-field cooled (ZFCM) modes were made on all samples in the range 20−2 K to check for long-range order.

RESULTS AND DISCUSSION

Synthesis and Structure of Polymeric HCTMCP^{2-} d-Block Complexes. The tetra-*n*-butylammonium salt of hexacyanotrimethylenecyclopropanediide, (n-TBA)$_2$(HCTMCP), was synthesized using the methods reported by Fukunaga.[14] The disodium salt is obtained by metathesis of the TBA product. Both the TBA^+ and the Na^+ salts were used as starting materials in the attempted preparations of transition metal coordination polymers. It was found that different products were formed depending on the HCTMCP salt that was used, although in all cases 2D coordination polymers were obtained.

Reaction of methanolic solutions of $M(NO_3)_2 \cdot xH_2O$, M = Mn^{II}, Co^{II}, Cd^{II} or $Fe(BF_4)_2 \cdot 6H_2O$, with solutions of [(n-TBA)$_2$(HCTMCP)] in acetonitrile, in a 1:1 molar ratio, yielded crystalline products in moderate yields. Structural characterization by X-ray crystallographic analysis showed the composition of the products to be (n-TBA)$_2$[M(HCTMCP)$_2$(H$_2$O)$_2$] (M = Mn, **1Mn**; M = Fe, **1Fe**; M = Co, **1Co**; M = Cd, **1Cd**) with microanalytical data supporting this formulation for the bulk material. The isomorphous family **1** crystallizes in the monoclinic space group $P2_1/c$ and contain one-half of the formula in the asymmetric unit.

The M^{II} centers in the structure of **1** are all equivalent and provide the 4-connecting nodes in a (4,4) square grid sheet topology (Figure 2). Each metal atom has a pseudo-octahedral *trans*-$M^{II}O_2N_4$ environment, coordinating to two *trans* aqua ligands and four nitrile-coordinated HCTMCP^{2-} ligands. Each HCTMCP^{2-} ligand acts in a bridging mode (**A** in Figure 1) and can be topologically considered as a linear connector with two of its six nitrogen atoms coordinated to two different metal centers, thereby forming M_4L_4 metallamacrocycles. The HCTMCP^{2-} ligands coordinate through two nitrogen atoms that belong to different $C(CN)_2$ substituents on the central C_3 ring. The average M−N distances are 2.23 Å (**1Mn**), 2.16 Å (**1Fe**); 2.11 Å (**1Co**) and 2.31 Å (**1Cd**). The intrametallacycle M···M distances along the

Table 1. Crystal Data for Complexes 1−5

	1Mn[a]	1Fe[a]	1Co	1Cd	2[a,b]	3Co[c]	3Zn[a]	4[c,d]	5
formula	$MnC_{56}H_{76}O_2N_{14}$	$FeC_{56}H_{76}O_2N_{14}$	$CoC_{56}H_{76}O_2N_{14}$	$CdC_{56}H_{76}O_2N_{14}$	$FeC_{18}H_{18}N_6O_3$	$Co_2C_{30}H_{24}N_{12}O_6$	$Zn_2C_{30}H_{24}N_{12}O_6$	$Mn_7C_{84}H_{84}N_{42}O_{42}$	$CuC_{16}H_6N_8$
FW	1032.25	1033.16	1036.24	1089.71	844.46	766.47	779.35	2738.51	373.83
crystal system	monoclinic	monoclinic	monoclinic	monoclinic	triclinic	triclinic	triclinic	rhombohedral	triclinic
space group	$P2_1/c$	$P2_1/c$	$P2_1/c$	$P2_1/c$	$P\bar{1}$	$P\bar{1}$	$P\bar{1}$	$R\bar{3}$	$P\bar{1}$
a, Å	10.9297(3)	10.9598(1)	10.9634(2)	10.9169(2)	8.6159(3)	7.8287(7)	7.7992(4)	21.3693(9)	8.7916(2)
b, Å	18.9720(11)	18.8191(2)	18.7609(5)	19.1132(2)	9.5297(3)	8.8368(7)	8.8762(5)	21.3693(9)	9.8806(2)
c, Å	13.9619(8)	13.9049(2)	13.8621(3)	14.0349(2)	12.6700(6)	12.4402(11)	12.4565(6)	69.219(2)	10.7660(3)
α, deg	90	90	90	90	84.027(1)	88.074(3)	87.501(2)	90	72.875(2)
β, deg	93.571(3)	93.516(1)	93.516(1)	93.681(1)	81.526(1)	81.756(3)	81.428(2)	90	89.817(1)
γ, deg	90	90	90	90	77.577(2)	85.783(6)	85.617(2)	120	64.172(1)
V, Å^3	2889.5(2)	2862.54(6)	2845.84(11)	2922.4(7)	1002.02(7)	849.19(13)	849.75(8)	27374(2)	795.91(3)
Z	2	2	2	2	1	1	1	9	2
D_{calc}, g cm^{-3}	1.186	1.199	1.209	1.238	1.399	1.499	1.523	1.495	1.560
μ, mm^{-1}	0.280	0.316	0.354	0.425	0.783	1.037	1.472	0.799	1.388
F(000)	1102	1104	1106	1148	436	390	396	12537	374
crystal size, mm	0.28 × 0.15 × 0.13	0.28 × 0.28 × 0.15	0.25 × 0.19 × 0.12	0.25 × 0.15 × 0.08	0.63 × 0.13 × 0.01	0.38 × 0.13 × 0.05	0.40 × 0.10 × 0.05	0.28 × 0.18 × 0.13	0.20 × 0.15 × 0.03
data collected	19038	33798	39919	34368	15647	10088	11357	106872	12602
unique data (R_{int})	7005 (0.067)	6780 (0.0647)	7097 (0.1855)	7161 (0.0585)	4708 (0.0858)	3682 (0.0861)	5154 (0.0215)	14812 (0.2775)	3829 (0.0579)
observed data [$I > 2\sigma(I)$]	4250	4547	3384	5265	3005	2268	4722	5611	3037
parameters	343	343	343	343	311	244	244	803	250
final $R1$, $wR2$ [$I > 2\sigma(I)$]	0.0497, 0.0811	0.0408, 0.0819	0.0674, 0.0967	0.0335, 0.0630	0.0573, 0.1154	0.1219, 0.2836	0.0340, 0.0703	0.0981, 0.1868	0.0405, 0.0773
$R1$,$wR2$ (all data)	0.1142, 0.1014	0.0854, 0.0968	0.1960, 0.1298	0.0620, 0.0700	0.1125, 0.1334	0.1813, 0.3069	0.0383, 0.0729	0.2470, 0.2758	0.0626, 0.0834
goodness of fit, S	1.048	1.056	0.990	1.021	1.014	1.167	1.118	0.989	1.045
$\Delta\rho_{min}$, $\Delta\rho_{max}$, e Å^{-3}	−0.696/0.382	−0.484/0.385	−0.642/0.720	−0.423/0.337	−0.570/0.650	−0.790/1.682	−0.357/0.369	−0.697/1.589	−0.467/0.520

[a] Hydrogen atoms attached to oxygen were refined at restrained distances of 0.86(1) Å from the oxygen atom. [b] Two of the three unique ethanol ligands are disordered over two positions and were modeled with freely refined occupancies. [c] Hydrogen atoms attached to oxygen could not be located and are therefore not assigned in the model. [d] The carbon atoms from one of the lattice HCTMCP dianions are disordered over two positions which were refined with fixed occupancies (50:50) and treated anisotropically.

dx.doi.org/10.1021/ic200591u |*Inorg. Chem.* 2011, 50, 6673–6684

$HCTMCP^{2-}$ bridges in the square (4,4) sheet are 11.78 (**1Mn**), 11.70 (**1Fe**), 11.66 (**1Co**), and 11.86 (**1Cd**) Å. A further two nitrile arms from each dianion, both belonging to the same $C(CN)_2$ substituent, accept hydrogen bonds from the aqua ligands that are attached to the same metal. The hydrogen bonding is therefore contained within the 2D sheets, and there are no strong intermolecular interactions between the parallel layers. The H···N distances lie in the range 1.94−2.15 Å across the whole structural series. Uncoordinated nitrile groups are known to act as good hydrogen bond acceptors both within structures of cyanometallate compounds and when the nitrile group is part of an organic ligand.[18] The HCTMCP dianion has itself been used in organic crystal engineering.[12f]

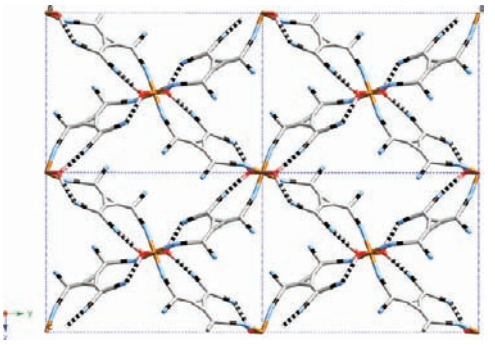

Figure 2. View along the crystallographic *a*-axis of the (4,4) network in the structure of **1Fe**, representative of the isomorphous series **1**. Hydrogen bonds between the coordinated water molecules and the $HCTMCP^{2-}$ dianions are represented by dashed bonds. The *n*-TBA cations are omitted for clarity.

The dianionic ligand exhibits a planar geometry with the most notable feature being the C−C and C−N bond distances which are only marginally longer those observed in charge-transfer salts containing $HCTMCP^{\bullet-}$ and $HCTMCP^{2-}$ (C−N approximately 1.15 Å in **1** and 1.11 Å in the CT donor−acceptor salts).[7] The coordination to the metal center does not appear to affect either the C−N bond distances or the geometry of the $HCTMCP^{2-}$ dianion to any significant extent.

To balance the negative charge of the (4,4) sheet there are *n*-TBA^+ cations present in the lattice (Figure 3). The alkylammonium cations reside above and below the square windows within the coordination polymer with two butyl chains, one from above and one from below, passing into each gap. There appear to be some weak interactions between the *n*-TBA^+ cations and the remaining free nitrile arms of the HCTMCP ligands with H···N distances of around 2.6 Å. The role of cations in templating anionic coordination networks of dicyanamide have been previously investigated, and it appears likely in this current case that the bulky *n*-TBA^+ cations have a significant effect on the network structure.[4e,19]

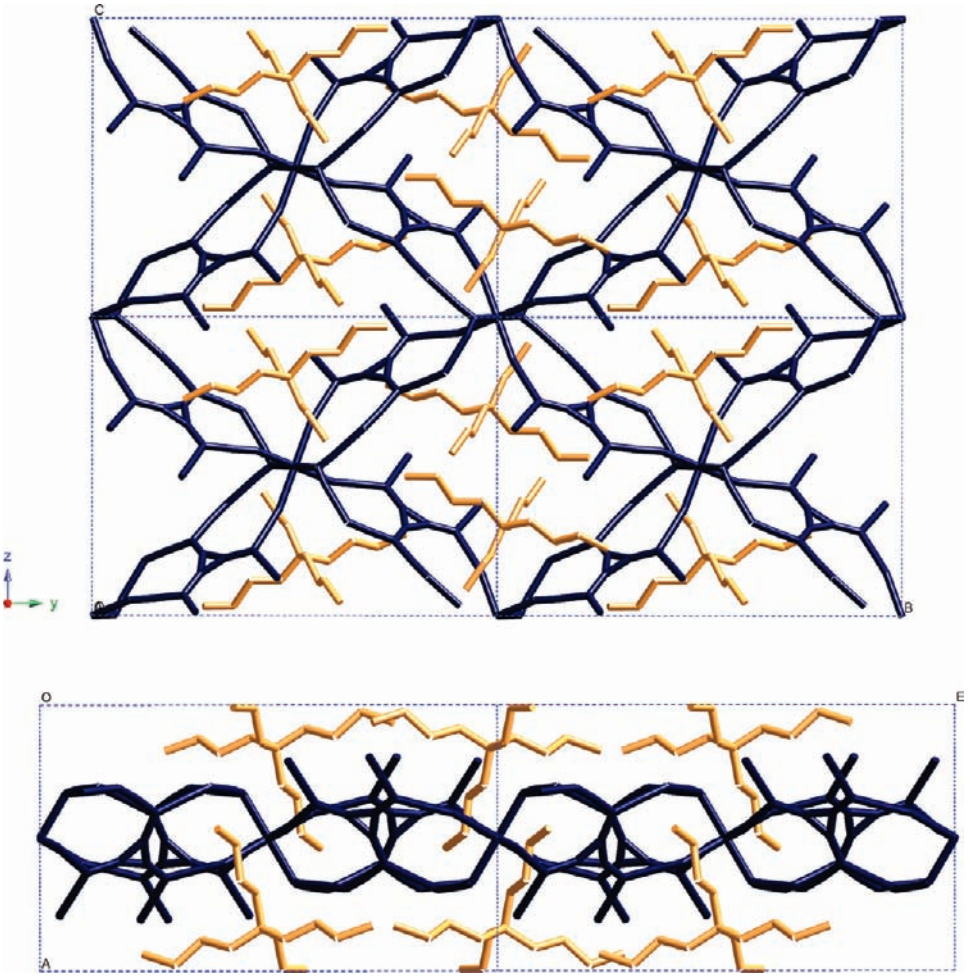

Figure 3. Tetra-*n*-butylammonium cations (shown in brown) reside above and below the square holes in the (4,4) sheets of **1Fe** (network shown in blue) viewed along (a) the *a*-axis, (b) the *c*-axis showing the protrusion of butyl chains into the square cavities.

dx.doi.org/10.1021/ic200591u |*Inorg. Chem.* 2011, 50, 6673–6684

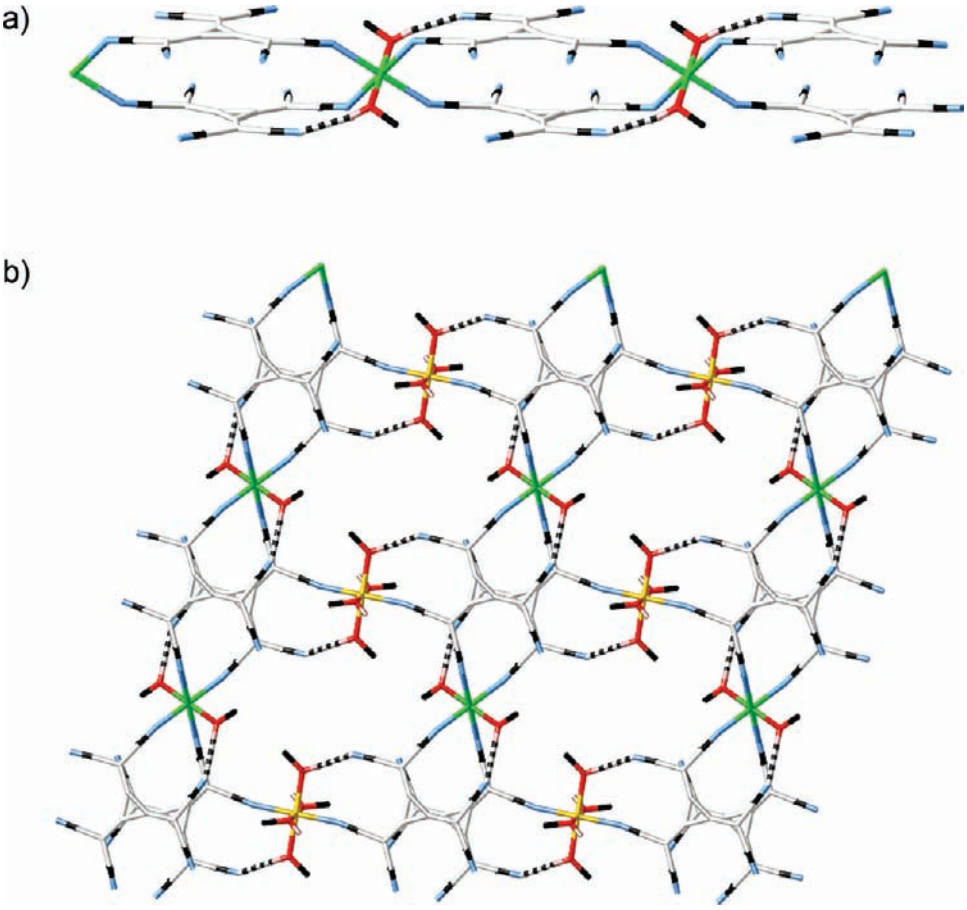

Figure 4. (a) Structure of **3Zn** broken down into 1D chains of $[Zn(HCTMCP)_2(MeOH)_2]^{2-}$ (shown in green) that are (b) connected by $[Zn(MeOH)_4]^{2+}$ units (shown in yellow) to form a 2D coordination polymer. Hydrogen bonds are represented as dashed cylinders. Methyl hydrogen atoms are omitted for clarity.

This templation effect of the cation is supported by the fact that use of the disodium salt, $Na_2HCTMCP$, as a starting material in the place of the tetrabutylammonium salt yielded a different series of products. Reaction of a solution of $Fe(ClO_4)_2 \cdot 6H_2O$ in ethanol with an aqueous solution of $Na_2HCTMCP$ in a 1:1 molar ratio yielded colorless needles that were determined to be $[Fe(EtOH)_4Fe(EtOH)_2(HCTMCP)_2]$ **2**. Analogous reactions between solutions of $Co(NO_3)_2 \cdot 6H_2O$ or $Zn(ClO_4)_2 \cdot 6H_2O$ in methanol with an aqueous solution of $Na_2HCTMCP$ yielded crystalline products that were found to be $[M(MeOH)_4M(MeOH)_2(HCTMCP)_2]$ (M = Co, **3Co**; M = Zn, **3Zn**) with a very similar structure to that of **2**. The reaction of $Mn(NO_3)_2 \cdot 4H_2O$ in a methanol/water solution gave a different structural motif to those of **2** and **3** in the compound $[Mn_3(HCTMCP)_2(H_2O)_{12}](HCTMCP) \cdot 6(H_2O)$ (**4**).

Compounds **2** and **3** are essentially isomorphous and exist in the triclinic space group $P\bar{1}$, with the larger coordinated solvent in **2** not affecting the overall structure. Detailed discussion below will be limited to **3Zn** for the sake of brevity. The asymmetric unit of **3Zn** contains halves of two unique octahedral metal centers, Zn(1) and Zn(2), one $HCTMCP^{2-}$ ligand, and three methanol molecules. The Zn(1) atom is coordinated to four separate $HCTMCP^{2-}$ ligands in the equatorial positions and two axial methanol ligands. The Zn(2) atom is coordinated by only two axial $HCTMCP^{2-}$ ligands and four equatorial methanol molecules.

The structure of the $[Zn(MeOH)_4Zn(MeOH)_2(HCTMCP)_2]$ polymer is a 2D-sheet; however, unlike in the structure of **1**, not all bridges between adjacent metal centers are equivalent. The 2D sheets in **3Zn** can be imagined to consist of 1D, anionic chain-like strands of $[Zn(MeOH)_2(HCTMCP)]^{2-}$, containing the Zn(1) atoms (Figure 4a). The HCTMCP ligands form a double bridge between the adjacent metal atoms with the coordinating nitrile arms being from separate $C(CN)_2$ groups, similar to 1D motifs that are observed in polymers containing dicyanamide.[20] In the structures of **2** and **3**, however, the C_3 rings of the two ligands within each bridging pair in 1D chains are parallel and in close proximity, with distances between ring centroids of 3.81 Å (**2**), 3.66 Å (**3Zn**), and 3.71 Å (**3Co**). This is indicative of a degree of π-stacking between the HCTMCP ligands. The separations between the metal atoms along the 1D chain are 11.39 Å (**2**), 11.36 Å (**3Zn**), and 11.37 Å (**3Co**). In addition to the coordinative interactions there are supporting hydrogen bonds along the chain between the ligated methanol molecules and the free nitrile arms of the HCTMCP ligands with O···N distances of 2.81 Å (**2**), 2.78 Å (**3Zn**), and 2.76 Å (**3Co**).

The 1D chains are connected by $[Zn(MeOH)_4]^{2+}$ groups, containing Zn(2), to form the 2D architecture (Figure 4b). Overall the topology of the structure can be viewed as a (4,4) sheet with the pairs of π-stacked HCTMCP ligands acting as the 4-connecting nodes, and the metal centers, which are both doubly and singly bridged by the ligands, simply acting as linear

dx.doi.org/10.1021/ic200591u |*Inorg. Chem.* 2011, 50, 6673–6684

connectors between the ligand pairs. Again, there are supporting hydrogen bonds between the methanol ligands and the uncoordinated nitrile arms. Two of the methanol molecules (one crystallographically unique) from the $[Zn(MeOH)_4]^{2+}$ units form hydrogen bonds within the square windows with O···N = 2.81 Å (**2**), 2.76 Å (**3Zn**), and 2.72 Å (**3Co**). The remaining two methanol ligands form hydrogen bonds to nitrile groups from parallel 2D sheets with interactions of a similar nature to those within the coordination polymers, O···N = 2.81 Å (**2**), 2.77 Å (**3Zn**), and 2.76 Å (**3Co**). The M−N bond lengths within and between the 1D chains are similar, with average values of 2.15 Å (**2**), 2.14 Å (**3Zn**), and 2.11 Å (**3Co**).

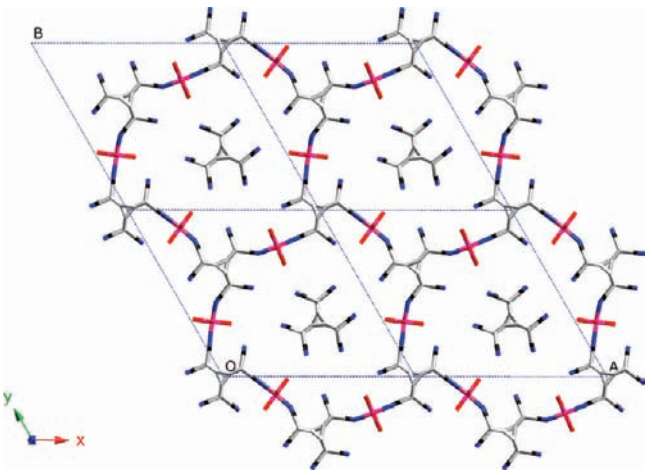

Figure 5. One crystallographically unique (6,3) sheet of $[Mn_3(HCTMCP)_2(H_2O)_{12}]^{2+}$, with associated $HCTMCP^{2-}$ counter-anions, in the structure of **4**, viewed along the *c*-axis. The structure comprises four unique, chemically identical sheets. Lattice water molecules have been omitted for clarity.

The product obtained when an analogous reaction to those yielding **2** and **3** was carried out with manganese is very different, namely, $[Mn_3(HCTMCP)_2(H_2O)_{12}](HCTMCP)\cdot 6(H_2O)$ (**4**). The Mn complex crystallizes in the rhombohedral space group $R\bar{3}$. The coordination networks within the structure are (6,3) sheets that propagate parallel to the *ab* plane (Figure 5). However, the complete structure comprises four crystallographically unique yet chemically and topologically identical sheets with the composition $[Mn_3(HCTMCP)_2(H_2O)_{12}]^{2+}$ that are charge balanced by uncoordinated $HCTMCP^{2-}$ anions that reside within the hexagonal windows. (The asymmetric unit contains three and a half Mn atoms). Each manganese atom adopts a slightly distorted octahedral coordination geometry with four aqua ligands and two $HCTMCP^{2-}$ ligands in mutually *trans* positions. The (6,3) sheet is constructed using the $HCTMCP^{2-}$ ligand as the three connecting node with one nitrile group from each $C(CN)_2$ substituent of the central C_3 ring coordinating to a Mn^{II} atom.

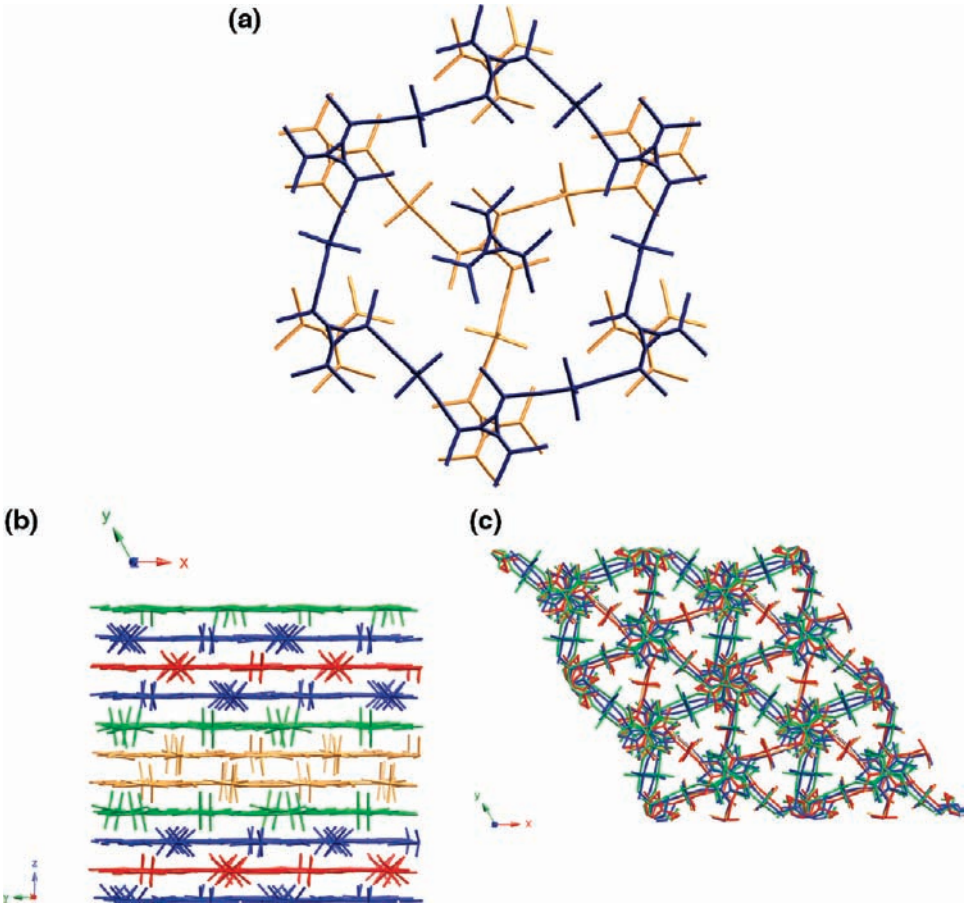

Figure 6. Crystal packing in the structure of **5**. (a) Two adjacent sheets showing the stacking of the uncoordinated $HCTMCP^{2-}$ above the ligated dianion. (b) View along the *a*-axis showing the alternating arrangement of the four crystallographically unique sheets. (c) View along the *c*-axis showing infinite stacks of HCTMCP as alternating ligated species and free anions.

dx.doi.org/10.1021/ic200591u |*Inorg. Chem.* 2011, 50, 6673–6684

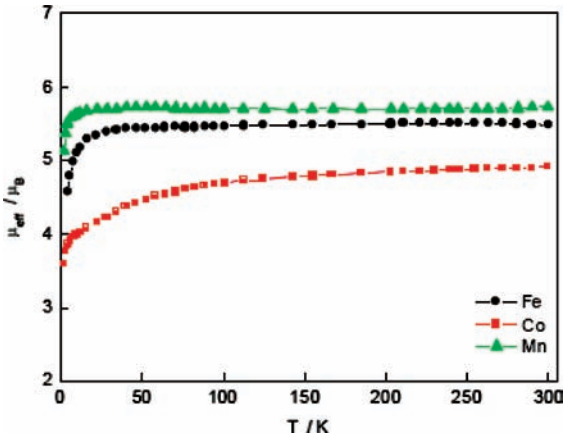

Figure 7. Plots of μ_{eff} versus temperature for **1Fe**, **1Co**, and **1Mn**, measured in an applied field of 1 T. The solid lines are not fitted curves.

The metal atom is linearly disposed (discounting the terminal aqua ligands) and therefore acts as a ditopic connector between the dianionic ligands with Mn···Mn distances in the range 10.69−11.04 Å. The bond lengths between the metals and ligands vary within the range 2.18−2.24 Å with the Mn−OH_2 distances in the range 2.14−2.24 Å.

The crystal packing **4** is quite complex (Figure 6). Adjacent polymeric layers are offset parallel to the *ab* plane such that the central C_3 units of the HCTMCP ligands are aligned with those of an interstitial $HCTMCP^{2-}$ anion on one face and one from another polymer on the other face (Figure 6a). The stacking of the HCMTCP groups through the structure is therefore arranged so that every third HCMTCP is uncoordinated. The HCTMCP units are twisted relative to each other, presumably to maximize the π-interactions between them. The distances between the C_3 ring centroids lie in the range 3.20−3.37 Å.

The uncoordinated $HCTMCP^{2-}$ anions are held in place by hydrogen bonding from the aqua ligands belonging to the polymeric layers that lie above and below. (Note, although the hydrogen atoms in the structure could not be experimentally located the O···N distances lie in the range 2.76−3.21 Å, with an average value of 2.90 Å, and are strongly indicative of hydrogen bonding interactions). The aqua ligands also hydrogen bond to the free nitrile arms of coordinated HCTMCP groups in adjacent layers, with the three free nitrile arms of each ligand all involved in intersheet interactions. The structure also contains a significant amount of lattice water that lies within triangular channels that run parallel to the *c*-axis (Figure 6c). These water molecules form extensive hydrogen bonding chains running through the channels, interacting with each other as well as with the aqua ligands and the HCTMCP units (both coordinated and free).

Magnetic Studies of $HCTMCP^{2-}$ Complexes. A survey of all the polymeric complexes (except **1Cd** and **3Zn**) was made by measuring μ_{eff} versus T (analogous to $\chi_M T$ vs T) over the temperature range 2−300 K in a field of 1 T. Magnetization measurements, in field-cooled (5 Oe) and zero-field cooled modes were made on all samples in the range 20−2 K to check for long-range order.

The compounds **1Fe**, **1Co**, and **1Mn** show μ_{eff} versus T plots that are in agreement with a lack of long-range magnetic order, as expected in weakly coupled systems having the long $\mu_{1,9}$-$HCTMCP^{2-}$ M-NC---CN-M bridging distances (Figure 7). The corresponding plots of χ_M^{-1} versus temperature (2−300 K) are all Curie−Weiss like ($\chi_M = C/(T-\theta)$) and show C and θ values of: 4.09 $cm^3\ mol^{-1}$ K and −0.2 K (**1Mn**); 3.80 $cm^3\ mol^{-1}$ K and −1.52 K (**1Fe**); 3.06 $cm^3\ mol^{-1}$ K and −8.5 K (**1Co**). The magnetic moments at 300 K (5.73 μ_B (**1Mn**); 5.48 μ_B (**1Fe**); 4.90 μ_B (**1Co**)) are all indicative of weak field octahedral ground states, the orbital degeneracy making those for Fe^{II} ($^5T_{2g}$) and Co^{II} ($^4T_{1g}$), greater than the spin-only values (4.90 μ_B and 3.87 μ_B respectively). The $M(HCTMCP)_2(H_2O)_2$ coordination sites thus produce an overall weak ligand field environment. In the case of **1Mn** the μ_{eff} remains constant at 5.73 μ_B between 10 and 300 K and then decreases slightly, below 10 K, to reach 5.12 μ_B at 2 K. Such behavior is expected for an orbitally nondegenerate $^6A_{1g}$ state undergoing zero-field splitting to yield Kramer levels $M_s = \pm 5/2, \pm 3/2, \pm 1/2$, the thermal depopulation of which gives the small, rapid decrease in the μ_{eff} below 10 K.[21] Any $Mn^{II}\cdots Mn^{II}$ spin−spin coupling is extremely weak as anticipated for the long $Mn^{II}\cdots Mn^{II}$ separation. No maximum in χ_m was detected down to 2 K, again indicative of very weak antiferromagnetic coupling. This is further substantiated by the Weiss constant, θ, being close to zero (see above). In **1Mn**, and other complexes, there was no sudden increase in μ_{eff} at low temperatures, as was present in binary species of type $[M^{II}(dca)_2]$, because of long-range magnetic ordered species.[4e] Further proof of a lack of order was, as indicated above, that the field-cooled (FCM) and zero-field cooled (ZFCM) magnetization versus temperature plots, below 20 K, did not show any bifurcation typical of long-range ordering.

Compound **1Fe** displays very little variation in μ_{eff} between ~30 and 300 K followed by a gradual decrease occurring below 30 K that reaches 3.59 μ_B at 2 K. Such behavior is indicative of an orbitally degenerate $^5T_{2g}$ state, with spin orbit coupling and low symmetry ligand−field effects causing a removal of degeneracy and splitting of the $^5T_{2g}$ state.[22] This leads to the temperature independent moment and the small decrease observed below ~20 K. Any exchange coupling is, again, likely to be very weak with the θ value of −1.52 K explainable by ligand-field splitting and zero-field splitting effects.

The data for **1Co**, including the Curie−Weiss behavior of susceptibilities (θ = −8.5 K) are very reminiscent of monomeric, octahedral Co^{II} species, that is, weakly to uncoupled Co^{II} centers.[22]

The products obtained from the reactions with $Na_2HCTMCP$, the Fe^{II} complex **2** and **3Co**, were also tested for their magnetic behavior. The value of μ_{eff} per Fe_2 for **2** is constant at 8.02 μ_B between 100 and 300 K (5.67 μ_B per Fe^{II}) and then decreases rapidly, below 100 K, to reach 2.96 μ_B at 2 K (Figure 8(left)). The corresponding χ_{Fe}^{-1} (per Fe_2) versus temperature plot is Curie−Weiss like ($\chi_M = C/(T-\theta)$) with θ = −4.21 K and C = 7.52 $cm^3\ mol^{-1}$ K. The room temperature value of μ_{eff} per Fe_2 is greater than the spin-only value for two $S = 2$ ions (6.93 μ_B) because of orbital degeneracy (formally $^5T_{2g}$ single ion terms) and spin orbit coupling effects.[22] The rapid decrease of μ_{eff} toward 2.96 μ_B at 2 K is due to very weak antiferromagnetic coupling, perhaps combined with zero-field splitting of the ligand-field ground state. Use of a Fisher chain $-2J\mathbf{S_1}.\mathbf{S_2}$ model for $S = 2$, eq 1, with zero-field splitting assumed as zero, yielded J = −0.67 cm^{-1} and $g = 2$.[23]

$$\chi = (Ng^2\mu_B{}^2/3k_BT)(S(S+1)\{(1+u)/(1-u)\}$$
$$u = \coth(-2JS(S+1)/k_BT) - (2JS(S+1)/k_BT) \quad (1)$$

where N = Avogadro's number, μ_B = Bohr magneton, g = Lande factor, $S = 2$, k_B = Boltzmann's constant.

dx.doi.org/10.1021/ic200591u |*Inorg. Chem.* 2011, 50, 6673–6684

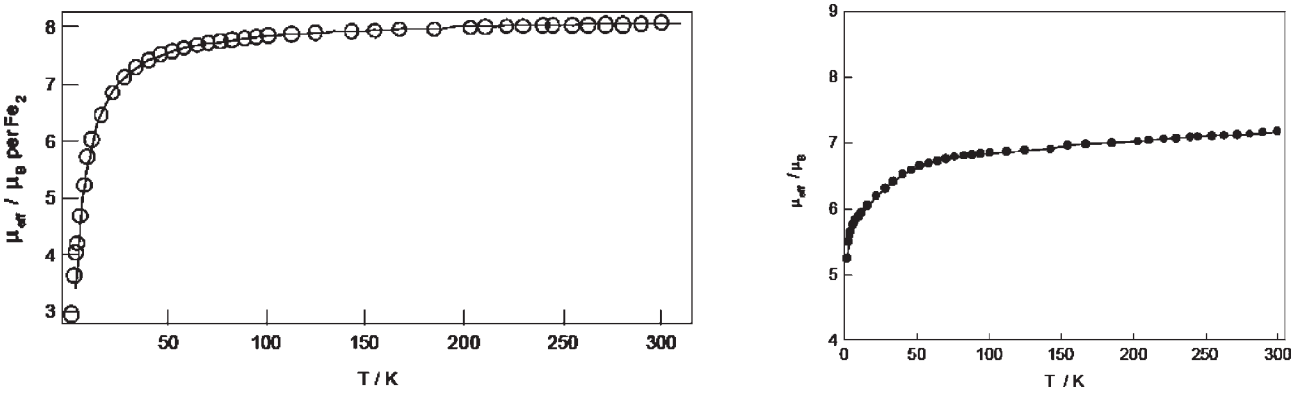

Figure 8. Plots of μ_{eff} (per M_2) versus temperature in a field of 1 T for (left) **2** and (right) **3Co**. The solid line for **2** is that calculated from eq 1; see text. The solid line for **3Co** just joins the points.

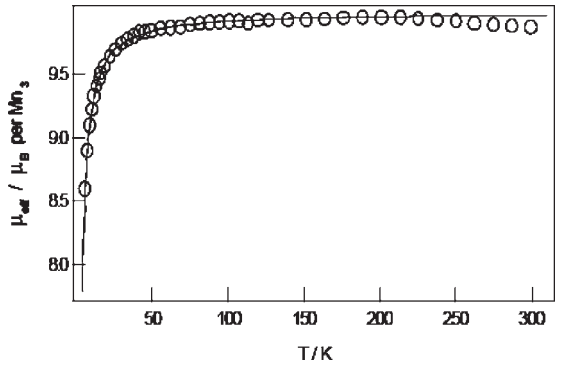

Figure 9. Plot of μ_{eff} versus temperature for **4** in an applied field of 1 T. The solid line is a best fit using the $S = 5/2$ 2D model.[24]

The magnetic moments for **3Co**, per Co_2, decrease from a value of 7.16 μ_B at 300 K (5.06 μ_B per Co^{II}) to reach 6.81 μ_B at 90 K (Figure 8(right)). There is then a more rapid decrease down to 5.23 μ_B at 2 K. This is typical behavior for octahedral Co^{II} ($^4T_{1g}$) centers with the temperature dependence arising from a combination of spin−orbit coupling and low symmetry ligand-field effects.[22] The Curie−Weiss constants are $\theta = -16.1$ K and $C = 6.7$ cm^3 mol^{-1} K (per Co_2) in the range 100−300 K. Very weak antiferromagnetic coupling is also possibly occurring, but this cannot be unambiguously identified since negative θ values arise from spin−orbit and ligand-field effects alone.[22]

The magnetic moment of **4** is essentially independent of temperature between 50 and 300 K at ∼9.9 μ_B, per $(Mn^{II})_3$ (5.72 μ_B per Mn^{II}) and then decreases rapidly below 50 K to reach 8.60 μ_B at 7.3 K (4.97 μ_B per Mn^{II}) (Figure 9). The Curie−Weiss constants obtained from the χ_m^{-1} versus T plot are $\theta = -1.05$ K and $C = 12.4$ cm^3 mol^{-1} K per $(Mn^{II})_3$. The use of a Heisenberg $(-2J\mathbf{S}_i.\mathbf{S}_j)$ $S = 5/2$ 2D model, eq 2, gave a good fit to the 10−210 K data with $g = 1.95$ and $J = -0.04$ cm^{-1}.[23,24] This behavior is typical for octahedral Mn^{II} ($^6A_{1g}$) centers with very weak antiferromagnetic coupling combined with zero-field splitting, the latter evident at temperatures below 50 K.[21] The zero-field splitting parameter, D, was not included in the analysis. It could be of similar magnitude to J.

$$\chi_{2D} = (35/12)Ng^2\mu_B{}^2/(k_BT)[1 + C_1x + C_2x^2 + C_3x^3 + C_4x^4 + C_5x^5 + C_6x^6) \quad (2)$$

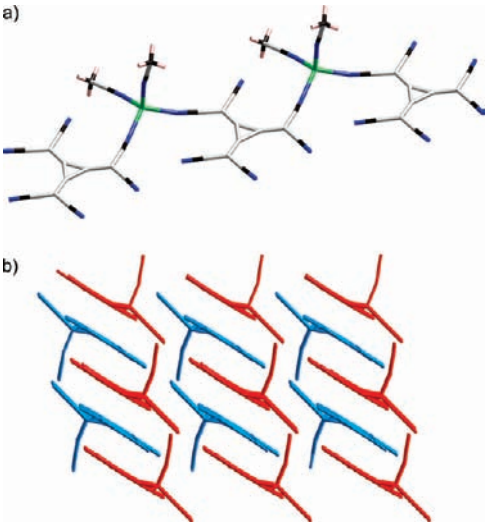

Figure 10. (a) Portion of the coordination polymer [Cu(HCTMCP)-$(MeCN)_2$], **5**. (b) The interdigitation between adjacent polymeric strands via weak π-interactions between the C_3 rings (hydrogen atoms omitted for clarity).

where $x = J/k_BT$, $C_1 = 23.33$, $C_2 = 147.78$, $C_3 = 405.45$, $C_4 = 8171.3$, $C_5 = 64968$, $C_6 = 15811$.

Synthesis, Structure, and Magnetism of the Radical Anion Complex [Cu^I(HCTMCP)$(MeCN)_2$], 5. The reaction of Cu-$(ClO_4)_2 \cdot 6H_2O$ with $K^+(HCTMCP^{\bullet -})$ in MeCN/MeOH afforded dark blue crystals that were determined by X-ray crystallography to be of the composition [Cu^I(HCTMCP)-$(MeCN)_2$], **5**. Microanalytical results confirm that the bulk material is of identical composition, and IR analysis shows characteristic peaks of the $HCTMCP^{\bullet -}$ radical at 2218 and 2190 cm^{-1}.[12b,c] It is interesting to note that although Cu^{II} was used in the reaction the product contains Cu^I. Potentially such a change could occur via a redox process between Cu^{II} and either the $HCTMCP^{\bullet -}$ species or the solvent methanol. To gain some idea on the mechanism, we made cyclic voltammetric measurements (see Supporting Information, Figure S6) on $(n\text{-TBA})_2$(HCTMCP), in MeCN, and found two reversible waves at $E_{1/2} = 0.45$ and 1.2 V relative to Ag/AgCl, the first being due to $HCMTCP^{2-} \rightleftharpoons HCMTCP^{\bullet -} + e^-$ and the second to $HCMTCP^{\bullet -} \rightleftharpoons HCTMCP + e^-$. Since the

dx.doi.org/10.1021/ic200591u |Inorg. Chem. 2011, 50, 6673–6684

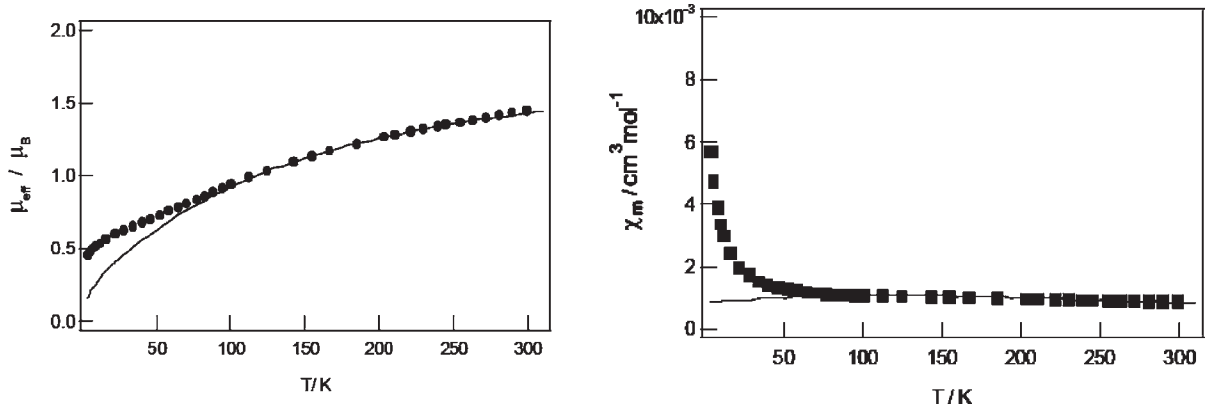

Figure 11. Plots for $[Cu^{I}(HCTMCP)(MeCN)_2]$, **5**, of (left) μ_{eff} versus T and (right) χ_M versus T. The solid lines represent best-fits using a $S = 1/2$ Fisher chain model[23] (low T divergence due to monomeric impurity).

$Cu^{II}(MeCN)_4/Cu^{I}(MeCN)_4$ $E_{1/2}$ potential (ref to Ag/AgCl) is 1.095 V (0.1 M $NaClO_4$ supporting electrolyte in MeCN), Cu^{II} will oxidize $HCMTCP^{2-}$ to form $HCMTCP^{\bullet-}$ and Cu^{I}. The reaction could also be followed by UV−visible spectroscopy such that the spectrum of deep-violet colored $K(HCMTCP^{\bullet-})$ has the same spectrum (550 sh, 600 and 680 nm; see Supporting Information Figures S7 and S8) as does $HCMTCP^{2-}$ plus $Cu^{II}(ClO_4)_2 \cdot 6H_2O$. The most likely mechanism of formation of **5**, from Cu^{II} plus $2K(HCTMCP^{\bullet-})$, is that the first mole equivalent of $HCTMCP^{\bullet-}$ radical reduces Cu^{II} to Cu^{I} and forms $HCTMCP^{0}$ while the second $HCTMCP^{\bullet-}$ coordinates to Cu^{I}.

Unfortunately, attempts to isolate other magnetically interesting metal complexes of $HCTMCP^{\bullet-}$, such as Mn^{II}, Fe^{II}, or Co^{II}, by reacting $K(HCTMCP^{\bullet-})$ with anhydrous MCl_2 in acetonitrile or tetrahydrofuran, were not successful despite repeated efforts.

$[Cu^{I}(HCTMCP)(MeCN)_2]$, **5**, crystallizes in the space group $P\bar{1}$ with a complete formula unit being present in the asymmetric unit (Figure 10a). The Cu^{I} atom adopts a distorted tetrahedral geometry with the $HCTMCP^{\bullet-}$ ligand bridging in a ditopic manner. The remaining two coordination sites are occupied by acetonitrile ligands. To our knowledge, this is the first example of a nitrile-bonded $HCTMCP^{\bullet-}$ metal complex. The $HCTMCP^{\bullet-}$ monoanion exhibits planar geometry with intraring C−C distances C101−C102 1.403(3), C102−103 1.406(3), C103−C101 1.411(3) Å (see Supporting Information for atom numbering and full details). These $C_{ring}-C_{ring}$ distances are similar to those in charge-transfer examples such as $[Fe(C_5Me_5)_2]$-$[HCTMCP^{\bullet}]$[12b,c] and are longer than in the $HCTMCP^{2-}$ complexes described above (av. 1.38 Å). The C−C and C−N bond lengths of the coordinated nitrile groups are not significantly different to those of the noncoordinated $HCTMCP^{\bullet-}$ group in charge-transfer species.[12b,c] The intrachain Cu···Cu distance is significantly longer than the shortest interchain Cu···Cu distance (9.96 vs 5.92 Å). There are weak $\pi\cdots\pi$ interactions between the C_3 rings of $HCTMCP^{\bullet-}$ ligands in parallel chains. These C_3 rings are significantly offset from each other with a separation between the ring centroids of 3.97 Å (the distance between the mean planes of the ligands is 3.12 Å). The weak interactions give rise to loosely connected 2D sheets by interdigitation of the 1D chains (Figure 10b). There are also very weak CH···nitrile interactions between the polymeric strands (H···N ∼ 2.6 Å).

Plots of μ_{eff} and χ_M versus temperature for $[Cu^{I}(HCTMCP)(MeCN)_2]$ are indicative of medium strength antiferromagnetic coupling (Figure 11). The broad maximum in χ_M between 70−300 K is typical of linear chain antiferromagnetic coupling behavior, with the rapid increase below 20 K indicative of monomeric $S = 1/2$ impurity, probably because of free $HCTMCP^{\bullet-}$ rather than any remnant Cu^{II}. The corresponding μ_{eff} values decrease from 1.44 μ_B at 300 K to ∼0.52 μ_B at 10 K, then more rapidly toward 0.42 μ_B at 2 K. Use of a Fisher chain $S = 1/2$ model gave a good fit to the 70−300 K data with $g = 2.05$ and $J = -110$ cm^{-1}.[22] The spin Hamiltonian and susceptibility equation used is that given in eq 1 but using $S = 1/2$.

It is intriguing to speculate whether the spins on $HCTMCP^{\bullet-}$ are coupled along the 1D chains, via the 9.96 Å $HCTMCP^{\bullet-}$ spaced Cu^{I} (diamagnetic) centers, in a σ-type fashion, or in a "through space" ligand $\pi-\pi$ fashion. Strong antiferromagnetically coupled "dimers" of $HCTMCP^{\bullet-}$ are known in charge-transfer compounds to generally lead to diamagnetic behavior with distances between the planes of adjacent anions being around 3.3 Å.[12b] There is one example, $[Fe(C_6H_3Me_3)_2]$-$[(HCTMCP^{\bullet-})_2]$, that showed weaker antiferromagnetic coupling, with a J of −495 cm^{-1} deduced from a $S = 1/2$ dimer model.[12c] The $\pi-\pi$ interactions that are present in the present compound are thus favored to be compatible with the exchange coupling observed. We do not observe any long-range magnetic order in this $HCTMCP^{\bullet-}$-coordinated 1D system, when measuring FCM and ZFCM in small DC fields, at 2−20 K, but this is perhaps not surprising in view of the $S = 0$ Cu^{I} centers, the dimensionality and the observed antiferromagnetic nature of the spin-coupling.

CONCLUSIONS

Eight new d-block coordination polymers containing the polycyano dianionic ligand $HCTMCP^{2-}$ have been synthesized and structurally characterized. The complexes are part of three structural families, all of which contain 2D coordination polymers. $(n\text{-TBA})_2[M(HCTMCP)_2(H_2O)_2]$ (**1**) (where M = Mn^{II}, Fe^{II}, Co^{II}, and Cd^{II}) consist of anionic polymers that are charge-balanced by bulky n-TBA cations that reside partially within the square windows of the (4,4) sheet. Syntheses using $Na_2HCTMCP$ as a starting material yielded complexes **2**, **3Zn**, and **3Co**, with the general form $[M(S)_4M(S)_2(HCTMCP)_2]$ (S = EtOH, **2**; S = MeOH, **3**). The neutral (4,4) sheets contain metal centers that are either singly or doubly bridged by the HCTMCP ligands, with an array of supplementary hydrogen

bonding involving the coordinated solvent molecules. The Mn^{II} compound, $[Mn_3(HCTMCP)_2(H_2O)_{12}](HCTMCP)\cdot 6(H_2O)$ (**4**), contains cationic (6,3) sheets that are charge-balanced by interstitial $HCTMCP^{2-}$ dianions. The layered structure contains significant $\pi-\pi$ interactions between the central C_3 rings of both the coordinated and the uncoordinated polycyano species. All of the compounds containing $HCTMCP^{2-}$ have been demonstrated to show weak antiferromagnetic coupling with no indication of long-range ordering. The weak coupling is a consequence of the long separations between adjacent metal centers and the poor superexchange pathways, as well as a lack of unpaired spins on the $HCTMCP^{2-}$ ligands. Magnetic order is thus not feasible. The 1D polymer $[Cu^{I}(HCTMCP^{\bullet-})(MeCN)_2]$ (**5**) displays medium strength antiferromagnetic coupling that is mediated by the radical monoanionic ligands, again without any long-range order evident. The lack of order probably results from factors such as the low spin of 1/2 on each $HCTMCP^{\bullet-}$ center, the lack of d-spin on the metal centers and the lack of a 3D network structure.

To be able to achieve new insights in to magnetic ordering in molecular magnetic materials containing polycyano bridging ligands, and make comparisons with the studies of tcne and tcnq systems, we need magnetic data on $HCTMCP^{\bullet-}$ when coordinated to d- or f- block ions that have large unpaired spin, such as $Mn^{II\text{ or }III}$, $Fe^{II\text{ or }III}$, Co^{II}, Gd^{III}, Dy^{III}. Unfortunately, to date, we have not been able to prepare these species. A full understanding of the weak exchange in the $HCTMCP^{2-}$ compounds **1** to **4**, and the medium antiferromagnetic exchange in $[Cu^{I}(HCTMCP^{\bullet-})(MeCN)_2]$ (**5**), will also require density functional theory (DFT) calculations and elucidation of $HCTMCP^{\bullet-}$ ligand singly occupied molecular orbital (SOMO) energy levels. These remain synthetic and calculational challenges for the future. Qualitatively, from the present findings, we would predict that exchange and long-range ordering in covalently bonded HCMTCP materials are weaker than in corresponding tcne and tcnq systems.

■ ASSOCIATED CONTENT

Supporting Information. Crystallographic information files (CIFs) containing X-ray data for compounds **1**−**5** and documentation containing selected bond lengths/angles alongside atomic labeling diagrams and full hydrogen-bonding parameters. Electrochemical CV plots and UV−visible spectral plots for compound **5**. This material is available free of charge via the Internet at http://pubs.acs.org.

■ AUTHOR INFORMATION

Corresponding Author

*E-mail: keith.murray@monash.edu (K.S.M.), stuart.batten@monash.edu (S.R.B.).

■ ACKNOWLEDGMENT

We thank the Australian Research Council (A.R.C.) and Monash University for funding. Dr. Alex Harris and Professor A. M. Bond are thanked for electrochemical studies and discussions.

■ REFERENCES

(1) (a) Batten, S. R.; Neville, S. M.; Turner, D. R. *Coordination Polymers: Design, Analysis and Applications*; Royal Society of Chemistry: Cambridge, U.K., 2008. (b) Herren, F.; Fischer, P.; Ludi, A.; Hälg, W. *Inorg. Chem.* **1908**, *19*, 956. (c) Ludi, A.; Güdel, H. U. *Struct. Bonding* **1973**, *14*, 1. (d) Bozorth, R. M.; Williams, H. J.; Walsh, D. E. *Phys. Rev.* **1956**, *103*, 572. (e) Ito, A.; Suenaga, M.; Ono, K. *J. Chem. Phys.* **1968**, *48*, 3597. (f) Miller, J. S. *MRS Bull.* **2000**, *25*, 60. (g) Goujon, A.; Varret, F.; Escax, V.; Bleuzen, A.; Verdaguer, M. *Polyhedron* **2001**, *20*, 1339. (h) Gadet, V.; Mallah, T.; Castro, I.; Verdaguer, M. *J. Am. Chem. Soc.* **1992**, *114*, 9213. (i) Greibler, W. D.; Babel, D. *Z. Naturforsch., Teil B* **1982**, *87*, 832.

(2) (a) Van Langenberg, K.; Batten, S. R.; Berry, J. K.; Hockless, D. C. R.; Moubaraki, B.; Murray, K. S. *Inorg. Chem.* **1997**, *36*, 5006. (b) Ferlay, S.; Mallah, T.; Vaissermann, J.; Bartolome, F.; Veillet, P.; Verdaguer, M. *Chem. Commun.* **1996**, 2481. (c) Bellouard, F.; Clemente-Leon, M.; Coronado, E.; Galan-Mascaros, J. R.; Gómez-Garcia, C. J.; Romero, F.; Dunbar, K. R. *Eur. J. Inorg. Chem.* **2002**, 1603. (d) Ohba, M.; Iwamoto, T.; Okawa, H. *Chem. Lett.* **2002**, 1046. (e) Inoue, K.; Imai, H.; Ghalsasi, P. S.; Kikuchi, K.; Ohba, M.; Okawa, H.; Yakhmi, J. V. *Angew. Chem., Int. Ed.* **2001**, *40*, 4242. (f) Miyasaka, H.; Matsumoto, N.; Re, N.; Gallo, E.; Floriani, C. *Inorg. Chem.* **1997**, *36*, 670. (g) Mallah, T.; Marvilliers, A.; Riviere, E. *Phil. Trans. R. Soc. London A* **1999**, *357*, 3139.

(3) (a) Enemark, J. H.; Holm, R. H. *Inorg. Chem.* **1964**, *3*, 1516. (b) Trofimenko, S.; Little, E. L., Jr.; Mower, H. F. *J. Org. Chem.* **1961**, *27*, 433. (c) Kohler, H. *Z. Anorg. Allg. Chem.* **1964**, *331*, 237.

(4) (a) Batten, S. R.; Robson, R.; Jensen, P.; Moubaraki, B.; Murray, K. S. *Chem. Commun.* **1998**, 439. (b) Miller, J. S.; Manson, J. L. *Acc. Chem. Res.* **2001**, *34*, 563. (c) Manson, J. L.; Kemety, C. R.; Huang, Q.; Lynn, J. W.; Bendele, G.; Pagola, S.; Stephens, P. W.; Epstein, A. J.; Miller, J. S. *Chem. Mater.* **1998**, *10*, 2552. (d) Kurmoo, M.; Kepert, C. J. *New J. Chem.* **1998**, *22*, 1515. (e) Batten, S. R.; Murray, K. S. *Coord. Chem. Rev.* **2003**, *246*, 103. (f) Kutasi, A. M.; Batten, S. R.; Moubaraki, B.; Murray, K. S. *J. Chem. Soc., Dalton Trans.* **2002**, 819. (g) Kmety, C. R.; Manson, J. L.; McCall, S.; Crow, J. E.; Stevenson, K. L.; Epstein, A. J. *J. Magn. Magn. Mater.* **2002**, *248*, 52. (h) Manson, J. L.; Kmety, C. R.; Epstein, A. J.; Miller, J. S. *Inorg. Chem.* **1999**, *38*, 2552.

(5) (a) Triki, S.; Sala-Pala, J.; Decoster, M.; Molinié, P.; Toupet, L. *Angew. Chem., Int. Ed.* **1999**, *38*, 113. (b) Triki, S.; Thétiot, S.; Vandevelde, F.; Sala-Pala, J.; Gómez-Garcia, C. J. *Inorg. Chem.* **2005**, *44*, 4086. (c) Thétiot, S.; Triki, S.; Sala-Pala, J.; Gohlen, S. *Inorg. Chim. Acta* **2005**, *358*, 3277. (d) Decoster, M.; Guerchais, J. E.; Le Mest, Y.; Sala-Pala, J.; Triki, S.; Toupet, L. *Polyhedron* **1996**, *15*, 195. (e) Thétiot, S.; Triki, S.; Sala-Pala, J.; Galán-Mascarós, J. -R.; Martínez-Agudo, J. M.; Dunbar, K. R. *Eur. J. Inorg. Chem.* **2004**, 3783. (f) Arthur, J. L.; Moore, C. E.; Rheingold, A. L.; Miller, J. S. *Inorg. Chem.* **2011**, *50*, 2735. (g) Turner, D. R.; Chesman, A. S. R.; Murray, K. S.; Deacon, G. B.; Batten, S. R. *Chem. Commun.* **2011**, in press, DOI:10.1021/1039c1cc11909E.

(6) (a) Miller, J. S.; Calabrese, J. C.; McLean, R. S.; Epstein, A. J. *Adv. Mater.* **1992**, *4*, 498. (b) Miller, J. S.; Vazquez, C.; Jones, N. L.; McLean, R. S.; Epstein, A. J. *J. Mater. Chem.* **1995**, *5*, 707. (c) Pokhodnya, K. I.; Petersen, N.; Miller, J. S. *Inorg. Chem.* **2002**, *41*, 1996. (d) Madalan, A. M.; Roesky, H. W.; Andruh, M.; Noltemeyer, M.; Stanica, N. *Chem. Commun.* **2002**, 1638. (e) Zhao, H.; Bazile, M. J.; Galán-Mascarós, J. R.; Dunbar, K. R. *Angew. Chem., Int. Ed.* **2003**, *42*, 1015. (f) Zhao, H.; Heintz, R. A.; Ouyang, X.; Dunbar, K. R.; Campana, C. F.; Rogers, R. D. *Chem. Mater.* **1999**, *11*, 736. (g) Heintz, R. A.; Zhao, H. H.; Xiang, O. Y.; Grandinetti, G.; Cowen, J.; Dunbar, K. R. *Inorg. Chem.* **1999**, *38*, 144.

(7) Miller, J. S. *Polyhedron* **2008**, *28*, 1596.

(8) Stone, K. H.; Stephens, P. W.; McConnell, A. C.; Shurdha, E.; Pokhodnya, K. I.; Miller, J. S. *Adv. Mater.* **2010**, *22*, 2514.

(9) Miyasaka, H.; Motokawa, N.; Matsunaga, S.; Yamashita, M.; Sugimoto, K.; Mori, T.; Toyota, N.; Dunbar, K. R. *J. Am. Chem. Soc.* **2010**, *132*, 1532.

(10) Miyasaka, H.; Motokawa, N.; Chiyo, T.; Takemura, M.; Yamashita, M.; Sagayama, H.; Harima, T.-H. *J. Am. Chem. Soc.* **2011**, *133*, 5338.

(11) Lopez, N.; Zhao, H.; Prosvirin, A. V.; Wernsdorfer, W.; Dunbar, K. R. *Dalton Trans.* **2010**, *39*, 4341.

(12) (a) Ward, M. D. *Organometallics* **1987**, *6*, 754. (b) Ward, M. D.; Fagan, P. J.; Calabrese, J. C.; Johnson, D. C. *J. Am. Chem. Soc.* **1989**, *111*, 1719. (c) Miller, J. S.; Ward, M. D.; Zhang, J. H.; Reiff, W. M. *Inorg. Chem.* **1990**, *29*, 4063. (d) Abrahams, S. C.; Bair, H. E.; Disalvo, F. J.; Marsh, P.; Deuring, L. A. *Phys. Rev. B* **1987**, *29*, 1258. (e) LePage, T. J.;

Breslow, R. J. *J. Am. Chem. Soc.* **1987**, *109*, 6412. (f) Lee, S. O.; Shacklady, D. M.; Horner, M. J.; Ferlay, S.; Hosseini, M. W.; Ward, M. D. *Cryst. Growth Des.* **2005**, *5*, 995. (g) Horiuchi, S.; Yamochi, H.; Saito, G.; Sakaguchi, K.; Kusunoki, M. *J. Am. Chem. Soc.* **1996**, *118*, 8604.

(13) Yates, M. L.; Arif, M. A.; Manson, J. A.; Kalm, B. A.; Burkhart, B. M.; Miller, J. S. *Inorg. Chem.* **1998**, *37*, 840.

(14) (a) Fukunaga, T. J. *J. Am. Chem. Soc.* **1976**, *98*, 610. (b) Fukunaga, T. J. U.S. Patent 3,963,769, 1976.

(15) Otwinowski, Z.; Minor, W. *Methods Enzymol.* **1997**, *276*, 301.

(16) Sheldrick, G. M. *Acta Crystallogr., Sect. A* **2008**, *64*, 112.

(17) Barbour, L. J. *J. Supramol. Chem.* **2001**, *1*, 189.

(18) (a) Gomm, P. S.; Underhill, A. E. *J. Chem. Soc., Dalton Trans.* **1971**, 334. (b) Krogman, K.; Hausen, H. D. *Z. Anorg. Allg. Chem.* **1968**, *358*, 67. (c) Turner, D. R.; Pek, S. N.; Batten, S. R. *Chem. Asian J.* **2007**, *2*, 1534. (d) Batten, S. R.; Hoskins, B. F.; Robson, R. *Inorg. Chem.* **1998**, *37*, 3432.

(19) (a) van der Werff, P. M.; Batten, S. R.; Jensen, P.; Moubaraki, B.; Murray, K. S. *Inorg. Chem.* **2001**, *40*, 1718. (b) van der Werff, P. M.; Batten, S. R.; Jensen, P.; Moubaraki, B.; Murray, K. S.; Cashion, J. D. *Cryst. Growth Des.* **2004**, *4*, 503. (c) van der Werff, P. M.; Batten, S. R.; Jensen, P.; Moubaraki, B.; Murray, K. S.; Tan, E. H. -K. *Polyhedron* **2001**, *20*, 1129.

(20) (a) Batten, S. R.; Jensen, P.; Kepert, C. J.; Kurmoo, M.; Moubaraki, B.; Murray, K. S.; Price, D. J. *J. Chem. Soc., Dalton Trans.* **1999**, 2987. (b) Jensen, P.; Batten, S. R.; Moubaraki, B.; Murray, K. S. *J. Solid State Chem.* **2001**, *159*, 352.

(21) Kennedy, B. J.; Brain, G.; Horn, E.; Murray, K. S.; Snow, M. R. *Inorg. Chem.* **1985**, *24*, 1647.

(22) (a) Mabbs, F. E.; Machin, D. J. *Magnetism and Transition Metal Complexes*; Chapman and Hall: London, U.K., 1973; (b) Reprinted as paperback by Dover Publications Inc: Mineola, NY, 2008. (c) Kahn, O. *Molecular Magnetism*; VCH: New York, 1993.

(23) Fisher, M. E. *Am. J. Phys.* **1964**, *32*, 343.

(24) Rushbrooke, G. S.; Wood, P. J. *Mol. Phys.* **1963**, *6*, 409.